Enabling Adaptive Cardio-Respiratory Biofeedback Training on Ubiquitous Hand-Worn Devices

Ruotong Yu*
Key Laboratory of Pervasive Computing, Ministry of Education, Department of Computer Science and Technology, BNRist
Tsinghua University
Beijing, China
Global Innovation Exchange
University of Washington
Bellevue, WA, USA
17800839246@163.com

Xintong Wu†
Department of Automation
Tsinghua University
Beijing, China
wuxt22@mails.tsinghua.edu.cn

Lily Sheng†
Department of Computer Science and Technology
Tsinghua University
Beijing, China
sheng.lily@outlook.com

Zihao Dong
Universiti Kebangsaam Malaysia
Bangi, Malaysia
a197779@siswa.ukm.edu.my

Yuntao Wang‡§
Department of Computer Science and Technology
Tsinghua University
Beijing, China
School of Computer Technology and Application
Qinghai University
Xining, Qinghai, China
yuntaowang@tsinghua.edu.cn

Yuanchun Shi‡
Department of Computer science and Technology, BNRist
Tsinghua University
Beijing, China
Intelligent Computing and Application Laboratory of Qinghai Province
Qinghai University
Xining, Qinghai, China
shiyc@tsinghua.edu.cn

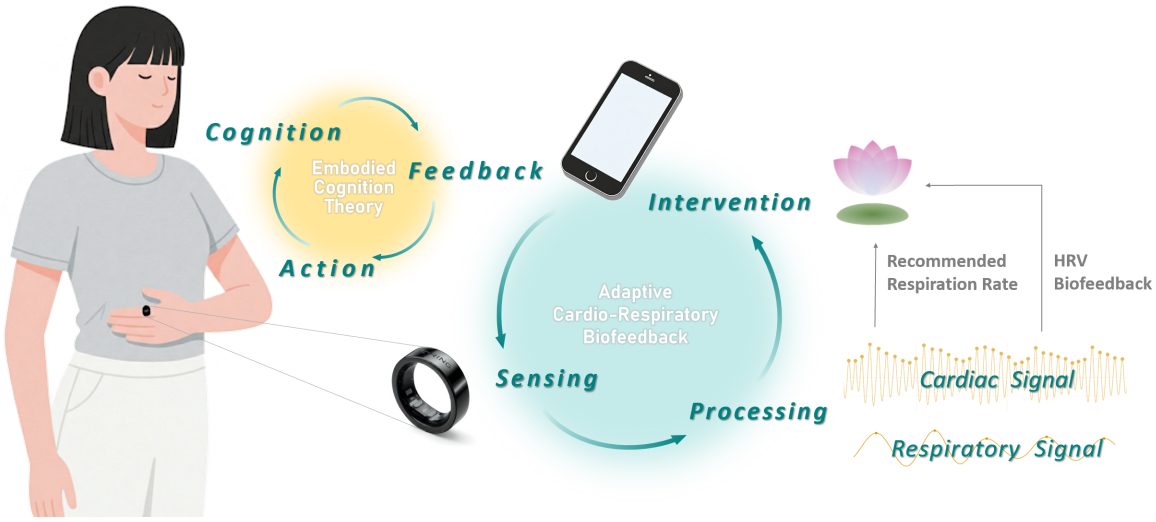

Figure 1: Our adaptive cardio-respiratory biofeedback system is built upon the interplay of two engineered loops. In the Action-Cognition Loop, the user connects their cognitive state to their physical breathing action, fostering embodied awareness. This is captured and augmented by the Signal-Biofeedback Loop, which uses wearable devices to translate physiological data into real-time guidance.

Abstract

We introduce an adaptive cardio-respiratory biofeedback system implemented on ubiquitous hand-worn devices such as smart watches and rings, enabling accessible and real-time physiological training outside clinical settings. Users place a hand on their abdomen to promote embodied awareness of breathing rhythms, while PPG and IMU sensors continuously capture cardio-respiratory signals. Unlike conventional open-loop biofeedback that delivers fixed breathing guidance irrespective of user response, our system employs a closed-loop adaptation: real-time physiological signals adjust breathing cues to optimize cardio-respiratory coupling, ensuring personalized training trajectories. This shift from static to adaptive guidance markedly improves user engagement and training efficacy. A user performance evaluation study further showed that adaptive biofeedback significantly boosts HRV, prolongs high-HRV states, and enhances user experience, demonstrating clear advantages over non-adaptive methods. Together, these findings position adaptive, hand-worn biofeedback as a promising approach for ubiquitous, user-centered mental health interventions.

CCS Concepts

• **Human-centered computing** → **Interaction paradigms**; **Interactive systems and tools**; *Interaction techniques.*

Keywords

Cardio-respiratory Coupling, HRV Biofeedback, Breathing Training, Hand-Worn Devices

ACM Reference Format:

Ruotong Yu, Xintong Wu, Lily Sheng, Zihao Dong, Yuntao Wang, and Yuanchun Shi. 2026. Enabling Adaptive Cardio-Respiratory Biofeedback Training on Ubiquitous Hand-Worn Devices. In *Proceedings of the 2026 CHI Conference on Human Factors in Computing Systems (CHI '26), April 13–17, 2026, Barcelona, Spain.* ACM, New York, NY, USA, 18 pages. https://doi.org/10.1145/3772318.3790488

1 Introduction

Cardio-respiratory Coupling (CRC) refers to the dynamic interaction and coordination between cardiac activity and respiratory rhythm at the physiological level [64]. A well-regulated CRC is associated with reduced anxiety levels, controlled physiological arousal, and positive outcomes in the management of chronic conditions such as chronic heart failure, hypertension, and chronic obstructive pulmonary disease (COPD) [29]. Heart Rate Variability Biofeedback (HRVB) for respiration training has been clinically demonstrated to enhance CRC. By guiding users to breathe at a resonant frequency (RF), HRVB activates the parasympathetic nervous system, increases HRV, and promotes coherence between cardiac and respiratory patterns [69].

Despite these established benefits, conventional HRVB protocols remain cumbersome: they rely on specialized equipment, assume a fixed resonant frequency, and often require a time-consuming calibration process to identify the individual's resonant frequency [48]. With the rise of wearable technologies, HRVB has become more accessible, yet most implementations continue to adopt rigid, fixed-paced breathing guidance. From a user experience perspective, this design has some shortcomings. Paced breathing at a fixed rate can feel uncomfortable and unnatural, which may discourage consistent use [13]. Furthermore, an individual's resonant frequency is not a stable metric, suggesting that a fixed-frequency approach is not only less effective but also fundamentally misaligned with the user's dynamic physiological state [16]. Therefore, dynamic monitoring of physiological indicators and adaptive adjustment of breathing guidance is crucial for providing a more natural and comfortable user experience while optimizing CRC and maximizing HRV outcomes.

Some researchers have recognized the limitations of fixed breathing guidance in HRVB and have proposed adaptive biofeedback models based on real-time physiological signals. For instance, certain systems monitor the user's breathing and provide guidance at a slower rate than the current rhythm [73]. Others adjust the breathing pace to be slower when HRV metrics indicate improved autonomic regulation [82]. These adaptive HRVB approaches have been shown to enhance user experience and improve CRC. For a personalized biofeedback system, it is important to regulate breathing guidance based not only on real-time HRV, which reflects the degree of cardio-respiratory coupling, but also on real-time breathing behavior, which indicates the user's engagement. However, many existing systems implement only one of these two adaptive mechanisms. Moreover, the majority of such studies rely on specialized equipment, making it difficult to extend HRVB training to everyday contexts.

Furthermore, while controlled breathing has long been recognized as an effective means of enhancing cardio-respiratory coupling and constitutes a central component of HRV biofeedback, current HRV biofeedback systems still face two major limitations. First, from an interaction design perspective, prior systems have explored various strategies to engage users in breathing practice. For example, replacing waveform displays with visual or auditory cues to make breathing perception more intuitive [51], or introducing gamified and VR-based tasks to foster immersion [21, 24]. Yet, few designs explicitly emphasize diaphragmatic breathing, despite evidence that it enhances the efficiency of deep breathing and

*Also with Key Laboratory of Pervasive Computing, Ministry of Education.
†Both authors contributed equally to this research.
‡Also with Qinghai University.
§Corresponding author.

CHI '26, Barcelona, Spain

ACM ISBN 979-8-4007-2278-3/26/04
https://doi.org/10.1145/3772318.3790488

strengthens parasympathetic activation. Second, most systems fail to monitor the extent to which users' actual breathing aligns with the prescribed guidance. Without such alignment feedback, users may deviate from the intended breathing pattern, undermining the effectiveness of training and reducing its long-term benefits.

Motivated by these gaps, we propose **the first hand-worn biofeedback system that dynamically adjusts breathing guidance frequency based on both real-time cardiac and real-time respiratory indicators**. Leveraging a hand-on-abdomen interaction, the device simultaneously captures HR and respiration to derive HRV and breathing behavior, which are then used to adapt biofeedback in real time.

To evaluate the effectiveness of the embodied interaction in enhancing diaphragmatic breathing, we first conducted a formative study with 16 participants, comparing the hand-on-abdomen posture with unconstrained free breathing. Results showed that the interaction enhanced diaphragmatic breathing by increasing both the amplitude and stability of respiratory cycles, while also improving user engagement. In parallel, we confirmed that smart ring and smartwatch sensors produced HR, HRV, and respiration rate measurements consistent with reference equipment, demonstrating sufficient reliability for daily-life biofeedback.

Building on the validated hand-on-abdomen interaction, we developed an adaptive biofeedback algorithm that continuously adjusts breathing guidance based on dual real-time physiological metrics. Heart rate variability is used to assess cardio-respiratory coupling, while respiration metrics capture user breathing alignment with the guidance. The system dynamically modulates the pacing of breathing cues to optimize both HRV enhancement and user adherence, providing a truly personalized training experience that responds to moment-to-moment physiological states.

To assess the efficacy of the adaptive biofeedback system, we conducted a controlled study with 48 participants performing structured biofeedback training across four conditions testing three independent variables: Visualization, Posture, and Guidance. Compared to the baseline fixed-rate biofeedback condition, the adaptive system produced higher sustained HRV, improved alignment with guided breathing, and greater user engagement, demonstrating the benefits of the hand-on-abdomen interaction and the integration of dual-factor real-time adaptation.

We summarize our key contributions as follows:

(1) The first hand-worn adaptive dual-factor biofeedback system that dynamically adjusts breathing guidance using both cardiac and respiratory indicators.

(2) Demonstration of a interaction paradigm where an intentional user posture simultaneously enhances embodied awareness and enables reliable biofeedback.

(3) Empirical evidence showing how the three key design factors—expressive visual feedback, embodied interaction, and dual-factor adaptive pacing—collectively influence biofeedback effectiveness by improving HRV rise, breathing alignment, physiological stability, affective experience, and user engagement, supporting scalable personalized stress regulation.

2 Related Work

2.1 Cardio-respiratory Coupling: Mechanisms and Relevance

Cardio-respiratory Coupling (CRC) is the dynamic synchronization between cardiac and respiratory rhythms, reflecting the deep physiological integration of these two systems [64]. This linkage is crucial for efficient physiological adaptation and maintaining homeostatic balance [26], and its effectiveness is a key indicator of a well-regulated autonomic nervous system (ANS) [15]. The neural foundation of CRC lies in the brainstem, where the respiratory center continuously modulates heart rhythm through sympathetic and parasympathetic (vagal) pathways [1]. During inhalation, sympathetic activity increases, accelerating the heart rate. Conversely, exhalation is dominated by parasympathetic activity, which decelerates the heart rate [10, 81]. This periodic, respiration-driven variation in heart rate is known as Respiratory Sinus Arrhythmia (RSA), the primary manifestation of CRC [29].

The magnitude of RSA, quantified in heart rate variability analysis as High-Frequency HRV (HF-HRV), is closely correlated with parasympathetic tone and is a primary measure of CRC quality [27]. An important metric used to assess this activity is the Root Mean Square of Successive Differences (RMSSD), a value reflecting the rapid, short-term heart rate fluctuations primarily mediated by the vagus nerve [9, 66]. Notably, the RMSSD is considered a more robust measure of parasympathetic (vagal) activity than RSA because it is less affected by fluctuations in respiration [37].

Strong and effective CRC helps to modulate the sympathetic "fight or flight" response, leading to reduced anxiety and better control over physiological arousal [31, 47, 75]. Clinically, enhancing CRC plays a beneficial therapeutic role in managing chronic conditions leading to better blood pressure regulation in hypertension [78], reduced cardiac workload in chronic heart failure [14], and improved exercise capacity in patients with chronic obstructive pulmonary disease [38]. Consequently, CRC is a key target for interventions like biofeedback and controlled breathing exercises, which are designed to consciously strengthen this vital physiological linkage [50].

2.2 Cardio-respiratory Sensing Techniques

Effective cardio-respiratory biofeedback depends on accurately monitoring both heart and breathing rates. The "gold standard" for measuring cardiac signals is electrocardiogram (ECG), which uses skin electrodes to detect the heart's electrical activity [70]. Phonocardiography (PCG) records acoustic signals [41] and seismocardiography (SCG) measures chest wall vibrations [18]. Photoplethysmography (PPG) has become the most widespread due to its simplicity, using optical sensors to measure blood volume changes [3, 71]. For monitoring breathing, respiration rate (RR) is a clinical parameter that measures the number of breaths per minute (bpm) [59]. Non-contact methods – infrared thermography [40], radar [44], and ultrasound [74] – offer remote monitoring. They are often sensitive to the subject's position or require complex setups [2]. Contact-based methods provide more direct measurements but may induce discomfort. Airflow sensing uses sensors near the face to analyze the differences in the properties of inhaled versus exhaled

air [30, 39, 43]. Other methods measure chest wall movement or torse movement using Respiratory Inductance Plethysmography (RIP) [80], strain gauge [23], piezoelectric sensor [84], or Inertial Measurement Units (IMUs) [6, 34, 36].

Crucially, respiratory rate can be derived indirectly from cardiac signals, as both ECG and PPG are modulated by breathing activity through RSA. Several studies have validated PPG as a viable replacement for ECG in many contexts [12, 28, 65]. This allows for the simultaneous extraction of heart and breathing data from a single sensor [17]. However, a drawback of PPG-derived respiration is its susceptibility to motion artifacts, which requires the person to be static for an accurate respiration rate measurement [33, 85].

The emergence of wearable devices–smart watches, wristbands, eye-wear, and smart rings–have allowed continuous health monitoring accessible by integrating PPG and IMU as standard components. While some consumer devices have included ECG [5], its requirement for multiple, stable electrical contacts limits widespread adoption compared to the cost-effective, and low-power nature of PPG and IMUs [19, 53, 68]. Since many hand-worn devices share the same sensors, ubiquitous systems allow individuals to choose the device they have at hand instead of requiring specialized devices, thus making it easier for individuals to keep track of their health.

2.3 Cardio-Respiratory Related Biofeedback Training Systems

Biofeedback is a therapeutic technique that provides individuals with real-time information on typically imperceptible physiological processes, enabling conscious self-regulation [32]. A study by Chittaro et al. [22] found that integrating real-time biofeedback into a VR experience significantly improved user relaxation and sense of presence compared to a placebo condition. Breathing biofeedback provides real-time data on respiratory rate and depth to increase awareness of natural breathing patterns. HRV Biofeedback provides direct feedback on the HRV signal. Cardio-respiratory biofeedback integrates both breathing biofeedback and HRV Biofeedback. Regardless of the specific form of biofeedback, the ultimate goal is to guide users toward a calm, balanced physiological state, and CRC is precisely a representation of this state. Since breathing is the most easily and consciously controllable pathway to reach such coherence, many HRV-based and breathing-based biofeedback systems incorporate some form of respiratory guidance. Studies have demonstrated that guided breathing protocols coupled with HRVB can lead to positive physiological outcomes, such as reduced depressive symptoms [57], reduced stress [45], and reduced blood pressure [52]. The most common approach for breathing guidance is fixed guidance, and more advanced systems implement adaptive guidance.

Fixed-paced (or open-loop) breathing guidance, which paces the user to breath at a single, constant rate. This rate, known as the resonant frequency, is the specific pace (typically 4.5–6.5 breaths/minute) that maximizes HRV amplitude [7]. The frequency is either individually determined before training or a standard rate is adopted. Pacer guides range from simple visuals like an expanding circle [58], to tactile feedback via physical expansion [73, 83] , to gamified mobile apps or digital therapeutics (DTx) [21, 54, 63].

While fixed-pace method is straightforward to implement, it suffers from several critical limitations. Research conducted by Steffen et al. [69] indicates that maximizing the benefits of guided breathing requires strict adherence to one's personal resonant frequency, as the effects are significantly reduced by a deviation of as little as one breath per minute. However, additional research has shown that an individual's resonant frequency is not static and can fluctuate over time or with changes in physiological state [16]. Moreover, the requirement to adhere to a fixed breathing rhythm can induce discomfort and feel artificial, which in turn compromises user adherence over the long term [13, 21]. These limitations highlight the fundamental flaws of a fixed-paced model, making it an suboptimal design for an effective, user-centered intervention.

Adaptive (or closed-loop) is a more robust paradigm that dynamically adjusts breathing guidance to the user's physiological state, nudging them toward CRC without disrupting their natural breathing tendencies. An example of such system is BioFidget where it provides both dynamic HRV and breathing biofeedback, using light cues integrated into a fidget spinner [51].

Table 1 compares existing biofeedback systems across adaptivity, feedback types, sensing modalities, and device form factors. The comparison reveals several key limitations in prior work:

- Although numerous systems integrate respiration or HRV feedback, fully adaptive biofeedback remains uncommon. The majority of existing solutions rely solely on fixed breathing guidance or single-modal biofeedback, lacking mechanisms that dynamically adjust to users' physiological responses.
- Even among adaptive approaches, most adjust to only a single physiological signal, missing the opportunity to leverage the complementary relationship between respiration dynamics and HRV modulation.
- Many prior systems depend on specialized or tightly coupled hardware ecosystems instead of ubiquitous, commodity platforms like smartphones, smartwatches, or smart rings. Consequently, they do not scale well and cannot support biofeedback experiences suited for everyday use.

To address these gaps, we introduce a hand-worn adaptive dual-factor biofeedback system that provides fully adaptive guidance by integrating both respiration and HRV signals. Our design further replaces specialized sensing hardware with ubiquitous IMU and PPG sensors embedded in hand-worn devices, enabling reliable biofeedback on a compact, everyday wearable platform. This approach supports scalable and seamless deployment of multimodal biofeedback in real-world settings.

3 System Design: Design Considerations and Rationale

Our study aims to integrate cardio-respiratory biofeedback training capabilities into ubiquitous hand-worn devices. We developed an adaptive biofeedback system implemented across two wearable form factors: a smart ring and a smart watch. The system provides real-time HRV and breathing feedback on cardio-respiratory coupling and dynamically adjusts breathing guidance based on both signals to ensure user engagement and comfort.

Table 1: Comparison of Biofeedback Systems for Respiration and HRV. We compare different systems across factors like adaptivity of breathing guidance (✓: Adaptive, ✗: Fixed), biofeedback type, sensing modality, input device to detect physiological signals, and output device to display biofeedback. The table is split into fixed breathing guidance systems (top section) and adaptive breathing guidance systems (bottom section).

Systems	Adaptivity	Biofeedback Type		Sensing Modality	Input Device	Output Device
		Respiration	HRV			
Breeze [67] and Jeong et al. [42]	✗	✓	✗	Breathing Sound	Smartphone	Smartphone
Breath of Life [21]	✗	✓	✗	Breathing Sound	Headphone	PC
Rockstroh et al. [62]	✗	✓	✗	IMU	VR Controller	VR
CardboardHRV [24]	✗	✗	✓	rPPG	Smartphone	VR
Qiu [11]	✗	✗	✓	PPG	Specialized Qiu Device	Specialized Qiu Device
Blum et al. [13] and Xu et al. [79]	✗	✗	✓	ECG	Polar Chest Strap	VR
Chao et al. [20]	✗	✗	✓	PPG	PPG	PC
Chittaro et al. [22]	✗	✓	✓	Elastic Girth Sensor and PPG	Elastic Girth Sensor and PPG	VR
Prabhu et al. [61]	✗	✓	✓	Elastic Girth Sensor and ECG	Elastic Girth Sensor and ECG	VR
Breathm [73]	✓	✓	✗	Barometric Pressure Sensor	Specialized Airbag	Specialized Airbag
ViBreathe [82]	✓	✗	✓	PPG	Specialized Soft Device	Specialized Soft Device
BioFidget [51]	✓	✓	✓	PPG, Hall Sensor	Specialized Fidget Spinner	Specialized Fidget Spinner
Ours	✓	✓	✓	IMU, PPG	Smart Ring	Smartphone

3.1 Embodied Interaction Posture: Rationale and Design

Because our system is deployed on a hand-worn wearable device, the quality of physiological sensing depends heavily on the user's physical posture. In early prototyping, we observed that free-hand positions introduce substantial motion artifacts in both IMU-based respiration tracking and PPG-based cardiac sensing, preventing stable respiration rate and HRV estimation for real-time adaptation. At the same time, prior work in embodied cognition and HCI shows that bodily engagement can shape perception and facilitate self-regulation. For instance, embodied cognition theory argues that cognitive processes are grounded in the body and are continuously shaped by sensorimotor experience [76], while Kirsh highlights how simple bodily configurations support attention and help externalize internal processes [46]. In breathing-related interactions specifically, Ma et al. [55] demonstrate that tactile awareness around the abdomen enhances users' perception of respiratory movement and improves breathing-related interaction quality.

Motivated by these insights, we designed an embodied interaction posture in which the user gently places one hand on the abdomen during biofeedback training. This posture serves two complementary roles. First, it stabilizes sensing: abdominal displacement during breathing produces a clean IMU pattern, and the hand's contact against the torso reduces gross arm motion, improving ring-based PPG signal stability. Second, it reinforces interoceptive attention. The tactile feedback of the hand following the rise and fall of the abdomen guides users' awareness toward respiratory movement, a core component of interoceptive experience.

3.1.1 Empirical Validation of Hand-on-Abdomen Posture . To validate our choice of adopting a hand-on-abdomen posture as the core embodied interaction in our system, we conducted a controlled experiment examining whether this tactile engagement enhances diaphragmatic breathing and increases interoceptive awareness. Prior work in embodied cognition and mindful breathing suggests that physical contact with the abdomen may strengthen awareness of respiratory movement, but it remains unclear whether such a minimal posture produces measurable physiological changes.

Method. Sixteen participants (10 female, 6 male; age 21–30) completed two counterbalanced breathing sessions: (1) an unconstrained free-breathing condition and (2) a condition where participants placed one hand on their abdomen. Each session is three minutes long. No explicit instructions on breathing technique or rhythm were provided. Thoracic and abdominal respiration were recorded using two HKH-11C belts placed at the ribcage and above the navel. After each session, participants completed selected items from three MAIA subscales (Noticing, Attention Regulation, Self-Regulation) using a 7-point Likert scale.

Measures. We evaluated both objective breathing metrics and subjective interoceptive experience. Objective measures included (1) the diaphragmatic-to-thoracic breathing ratio and (2) respiration rate, computed from dual respiratory belts placed at the chest and abdomen. To assess subjective experiential changes, we used selected items from the Multidimensional Assessment of Interoceptive Awareness (MAIA) [56], a widely used instrument for quantifying interoception in mindfulness and somatic-awareness research. MAIA conceptualizes interoception as a set of distinct but interrelated abilities, including detecting internal sensations, sustaining attention on bodily processes, and using bodily cues to support emotional and mental self-regulation. Because our goal was to capture immediate experiential effects induced by hand placement, we

focused on three MAIA dimensions most relevant to moment-to-moment breathing practice: *Noticing* (awareness of internal sensations), *Attention Regulation* (ability to direct and maintain attention on the body), and *Self-Regulation* (using bodily cues to regulate one's state). Participants rated each item using a 7-point Likert scale.

Findings. Placing the hand on the abdomen significantly increased diaphragmatic breathing intensity (2.34 ± 1.58 vs. 1.12 ± 0.64; $p < 0.01$) and reduced respiration rate (15.69 ± 5.40 vs. 19.51 ± 2.69 bpm; $p < 0.05$). Participants also reported significantly higher Noticing, Attention Regulation, and Self-Regulation scores ($p < 0.01$ for all). These results demonstrate that even minimal tactile contact with the abdomen strengthens interoceptive focus and promotes deeper, more stable diaphragmatic respiration.

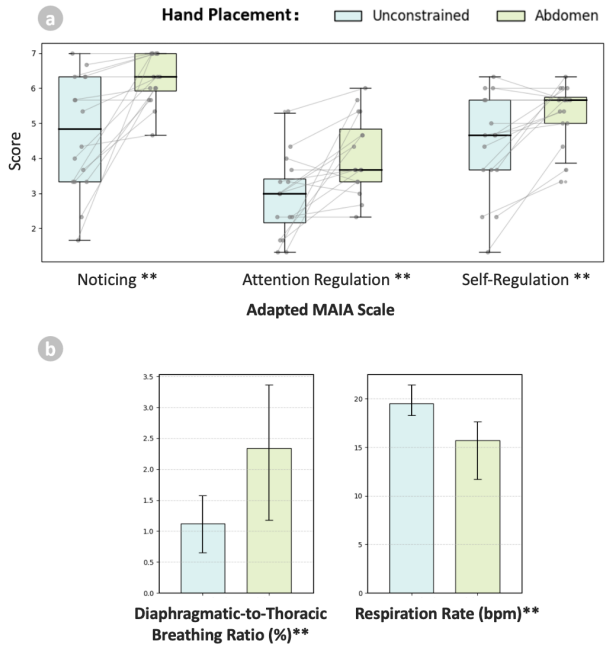

Figure 2: (a) Diaphragmatic-to-thoracic breathing ratio and respiration rate under unconstrained and abdomen conditions. (b) Adapted MAIA scale scores. Each box represents the mean score of three items within the same dimension. Horizontal lines (—) indicate the median. Asterisks denote statistically significant differences between conditions based on the Wilcoxon signed-rank test (*p < 0.05, **p < 0.01, ***p < 0.001).

Design Implications. These findings empirically support the use of a hand-on-abdomen posture as a core interaction mechanism. The posture simultaneously enhances embodied awareness and improves respiration signal quality, enabling reliable IMU-based breathing detection on the hand-worn device. Moreover, the average respiration rate observed under this posture informed the initial breathing guidance parameters used in our adaptive biofeedback algorithm.

3.2 Adaptive Strategy Design: Dual-Factor Closed-Loop Mechanism

With the embodied interaction posture introduced in the previous subsection, our ring-based system can simultaneously capture respiration cycles from IMU signals and cardiac intervals from PPG signals. To enable real-time adaptation on wearable-grade data, we use lightweight preprocessing: IMU signals are band-pass filtered and peak-detected to derive breathing cycles, and PPG signals are band-pass filtered to extract beat-to-beat intervals for HRV (RMSSD). Both respiration rate and HRV are computed using a 30 s sliding window updated every 5 s, providing a balance between responsiveness and physiological stability. With these two physiological channels available from a single compact wearable, we introduce a dual-factor adaptive biofeedback mechanism that integrates real-time respiration rate tracking with longer-term HRV trends to continuously personalize the breathing guidance.

The remainder of this subsection presents the rationale, mathematical formulation, and multi-layer control architecture of this adaptive strategy.

3.2.1 Respiration Rate as Short-Term Entrainment and Stability Gate. Although respiration rate is estimated using the same 30 s window as HRV, it is used as a *short-term reliability indicator*. Since our system does not measure each user's personal resonant frequency, we must initialize the guided breathing rate carefully. Prior work places resonant frequency between 4.5–6.5 bpm [69], and some systems recommend starting with the user's natural breathing cycle plus an additional 0.5 s [73]. Based on these insights and the average natural respiration rate (≈15 bpm) observed in Section 3.1.1, we set the initial guidance cycle to 4.5 s.

For each new window t, we compute the guided breathing rate GR_{target} and compare it with the user's actual respiration rate RR_t:

$$E_t = |RR_t - GR_{\text{target}}| \tag{1}$$

A window is considered "entrained" if:

$$E_t < 1 \text{ bpm}$$

Only when three consecutive windows (40 s) satisfy this condition does the system consider the user to be stably following the guidance. **Thus, respiration rate provides a short-term gate that determines whether adaptation is allowed, ensuring comfort and preventing premature adjustments.**

3.2.2 HRV as Long-Term Physiological Optimization Signal. In contrast, HRV is used to determine the *direction* of adaptation. We compute RMSSD over the same 30 s window and evaluate a multi-window trend rather than relying on a single-window value:

$$\Delta HRV_t = HRV_t - \widetilde{HRV}_{t-1}, \tag{2}$$

where $\widetilde{HRV}_{t-1}$ is an exponential moving average representing the user's physiological baseline over the past 2 minutes. If respiration rate stability is satisfied, HRV then determines whether slowing the breathing rate yields improved autonomic engagement:

$$GR_{\text{target}} = \begin{cases} GR_{\text{target}} - \delta, & \text{if } \Delta HRV_t > \theta_{\uparrow}, \\ GR_{\text{target}} + \delta, & \text{if } \Delta HRV_t < -\theta_{\downarrow}, \\ GR_{\text{target}}, & \text{otherwise.} \end{cases} \quad (3)$$

To avoid oscillation, we enforce a minimum 30s interval between updates of GR_{target}.

3.2.3 Multi-Rate Closed-Loop Control. Even though both respiration rate and HRV are derived from 30 s windows and updated every 5 s, their decision roles differ fundamentally:

Table 2: Roles of Respiration Rate and HRV in the dual-factor adaptive mechanism.

Component	Scale	Decision Basis	Function
Respiration Rate	Short-term	Single-window assessment	Evaluates entrainment and breathing stability in real time. Serves as a gate that determines whether adaptation is permitted, preventing adjustments when the user is not following the guidance.
HRV	Long-term	Multi-window trend	Determines the direction of adaptation by assessing whether slowing or speeding the breathing rate improves autonomic engagement. Only updates when respiration rate stability is maintained.

This produces a natural two-timescale system: Respiration rate governs *permission to adapt*, while HRV governs *direction of adaptation.*

3.3 Visualization Design: Lotus Flower and Lotus Leaf

Our dual-factor adaptive strategy requires two interactive, real-time visual feedback components: one reflecting the user's moment-to-moment HRV and another guiding breathing at a personalized pace. Both elements are continuously updating responsive components that respond directly to the user's physiological signals during use. The two elements are implemented in the form of a lotus-based interfaced composed of:

Lotus Flower (HRV Biofeedback): The lotus flower dynamically expands and contracts according to the user's HRV-derived augmented respiration signal, providing immediate visual feedback on autonomic activity and cardio-respiratory coupling. Its motion directly mirrors real-time physiological changes, enabling users to perceive and adjust their state moment by moment.

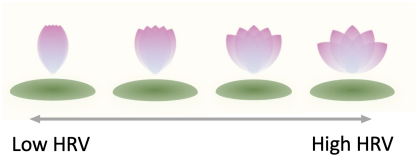

Figure 3: The lotus flower reflects the user's HRV state: higher HRV results in a more open lotus, while lower HRV causes the lotus to close.

Lotus Leaf (Adaptive Breathing Guidance): The lotus leaf functions as the core breathing guidance cue: its opening signals abdominal expansion during inhalation, and its closing signals abdominal contraction during exhalation. The tempo and amplitude of the leaf's motion adapt dynamically to the user's real-time breathing pattern and the system's dual-factor adaptive model. Serving as the primary interactive cue, the leaf guides users to synchronize their breathing with the recommended target pace.

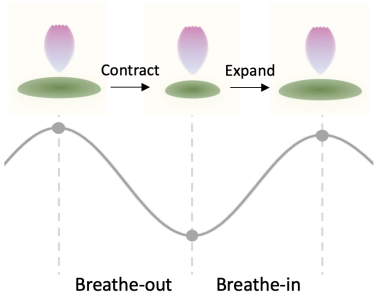

Figure 4: The lotus leaf guides the user to breathe: When the leaf opens, it prompts abdominal expansion for inhaling; when it closes, it prompts contraction for exhaling.

We chose the lotus as our visualization form factor because nature-inspired interfaces have been shown to promote calmness, reduce attentional demand, and support emotional receptivity—all essential for effective biofeedback training. A study by Barreiros et al. [8] shows that representing machine states through gentle, ambient natural cues—such as leaf color or foliage density—helps users remain informed without being overloaded or stressed by intrusive alerts.

Flower-like, organic forms have been known to evoke relaxation and positive affect, and the lotus specifically carries cross-cultural associations with breathing regulation, balance, and meditative clarity. Drawing on research indicating that warm-colored flowers (specifically red and yellow) elicit significantly higher parasympathetic activity and physiological relaxation compared to neutral colors [77], we selected the color of the lotus to be pink to maximize the visualization's beneficial effects.

Many existing biofeedback systems have embedded their biofeedback cues directly into immersive nature scenes, using the rhythm of elements like ocean waves to guide users' breathing [13] and using the growth of a virtual tree [20] or flower [79] to reflect HRV. By grounding real-time physiological feedback in gentle, organic motion rather than abstract geometric forms, the lotus interface provides a calm, intuitive, and emotionally supportive user experience aligned with the goals of stress-regulation and adaptive biofeedback.

4 Integrated System Architecture and Signal Quality Assessment

Our system integrates embodied interaction, dual-factor physiological feedback, and adaptive breathing guidance into ubiquitous hand-worn devices. The system provides real-time HRV and breathing feedback on cardio-respiratory coupling and dynamically adjusts breathing guidance based on both signals to ensure user engagement and comfort.

4.1 System Implementation

4.1.1 Hardware Setup. We used the τ-Ring [72], which incorporates several key modules, including the IMU (ICM-42688P) and PPG (GH 3026) sensors, with a sampling frequency set to 25Hz. Our smart watch hardware prototype consists of an Arduino Uno board, a 6-axis IMU (MPU6050), and a PulseSensor, all housed within a custom 3D-printed casing. The MPU6050 provides both accelerometer and gyroscope data, while the PulseSensor monitors heart rate. The system samples data at 25Hz, ensuring continuous and synchronized data collection.

4.1.2 Data Streaming and Signal Processing. Both the ring and smart watch systems support real-time data acquisition and transmission. To facilitate data transfer to computers or mobile devices, we developed a mobile application and a web application. The ring communicates with the mobile app via Bluetooth, streaming IMU and PPG data in real time. The data is then preprocessed. IMU signals are band-pass filtered and then go through peak detect to extract breathing cycles. PPG signals are band-pass filtered to extract beat-to-beat intervals for HRV (RMSSD).

4.1.3 Adaptive Feedback System. Using the calculated physiological signal, we implement a cardio-respiratory biofeedback strategy (detailed in Section 3.2) to compute optimal breathing guidance, which is visually represented through a lotus flower interface. Similarly, the smart watch transmits IMU and PPG data to the web application through a computer interface, where the same biofeedback strategy calculates and displays the recommended breathing patterns in real time.

4.2 Signal Quality Assessment

4.2.1 Experimental Setup. We evaluated the performance of our ring and smart watch by comparing their physiological measurements against established benchmarks. We collected data from 10 participants who simultaneously wore the ring, the smart watch, and reference devices while performing hand-to-abdomen breathing[1]. HR and HRV were validated using the VIVALINK ECG patch. Respiration rate was compared with signals from a HKH-11C piezoelectric respiratory belt. Both devices are well-established and widely accepted for their respective measurement applications, making them suitable benchmarks for our validation study.

4.2.2 Accuracy Across Physiological Signals. For HR estimation, we compared two approaches: Fast Fourier Transform (FFT) and filtered peak detection. The peak detection method demonstrated superior performance in this task. Based on the detected peaks, we calculated HRV using the RMSSD (Root Mean Square of Successive Differences) index derived from peak-to-peak intervals. We also compared RMSSD with SDNN (Standard Deviation of Normal-to-Normal Intervals) and found that the two metrics were comparable. We ended up using RMSSD for the final calculation of HRV since it is considered to be a robust measure of parasympathetic activity.

Respiration rate was primarily detected using motion signals from IMU sensors. In addition to traditional IMU-based methods, we explored the use of PPG signals. Typically considered noise in stationary measurements, motion artifacts in PPG were treated as useful signals in this context.

Our comparison showed that while PPG-based respiration estimation yielded reasonable results, it was still outperformed by the IMU-based approach (Table 3). Therefore, we adopted the IMU method for respiration detection in our subsequent system design.

Table 3: Comparison of error metrics between smart watch and smart ring across different tasks and methods.

Smart Watch				Smart Ring			
Task	**Method**	**MAE**	**MAPE**	**Task**	**Method**	**MAE**	**MAPE**
HR (FFT)	PPG	4.24	6.03%	HR (FFT)	PPG	6.28	9.19%
HR (Peak)	PPG	2.53	2.91%	HR (Peak)	PPG	1.61	2.35%
HRV	PPG	9.62	14.32%	HRV	PPG	9.07	13.5%
RR	PPG	0.743	9.97%	RR	PPG	0.452	6.06%
RR	IMU	0.343	4.50%	RR	IMU	0.236	3.11%

4.2.3 Summary of Findings. Across the tasks of HR, HRV, and respiration rate detection, the ring consistently outperformed the smart watch. We attribute this to two main factors:

(1) In the hand-on-abdomen posture, the ring experiences greater displacement due to diaphragmatic breathing, which enhances the accuracy of respiration detection.

(2) For HR signal accuracy, we believe the PPG sensor in our prototype smart watch did not maintain as consistent skin contact as the ring's sensor, leading to relatively lower signal quality.

Based on these findings, we conclude that both the ring and smart watch PPG sensors are suitable for HR and HRV detection, and either IMU or PPG sensors can be used for respiration rate estimation. However, given the lower error rates, we selected the ring as the preferred device—using its PPG sensor for HR and HRV and its IMU sensor for respiration detection—to achieve optimal overall performance in our system.

5 User Study: Biofeedback Training Effectiveness Evaluation

In this study, we aim to assess whether ring-based adaptive cardio-respiratory biofeedback improves the quality of biofeedback training, enhances user engagement, and reduces short-term stress compared to a baseline condition. To disentangle the contributions of key system components—including the lotus-based visualization, the embodied hand-on-abdomen posture, and the dual-factor adaptive feedback mechanism—we implemented a four-condition

[1]The study protocol was reviewed and approved by the university ethics review board. The compensation was consistent with the average earning of workers in the community where the study took place.

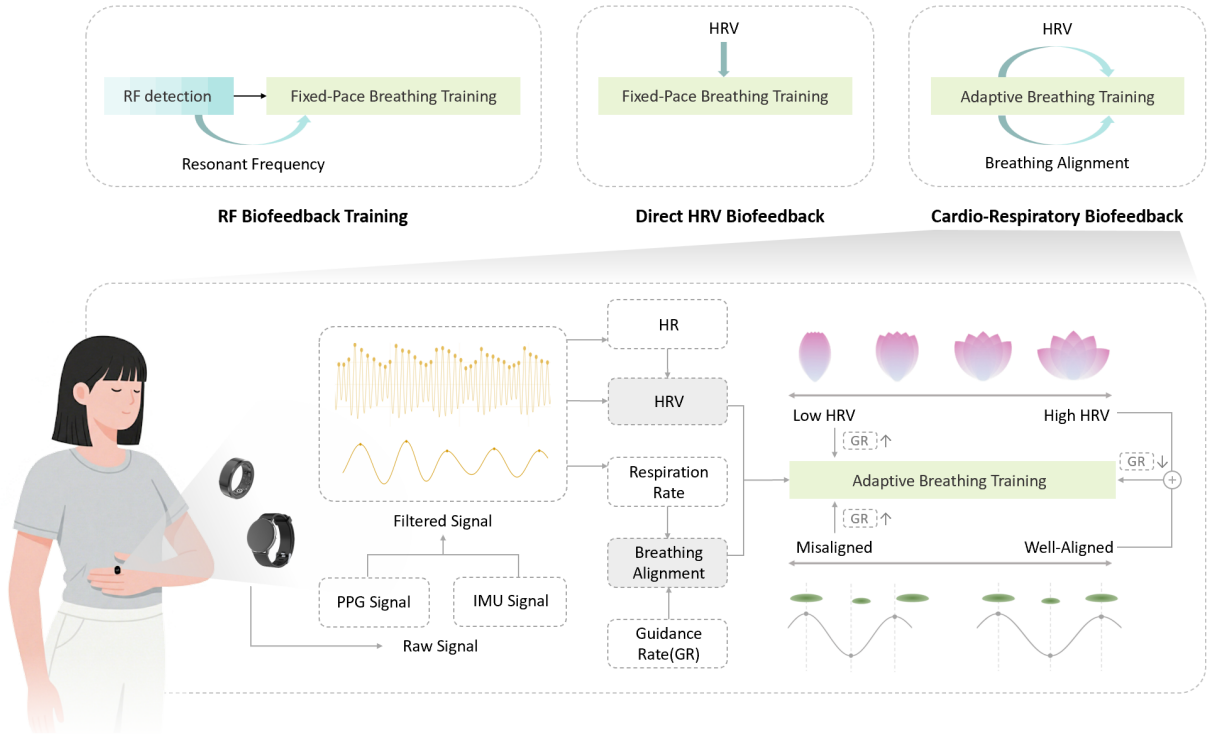

Figure 5: Cardio-Respiratory Biofeedback Training System Design. Our cardio-respiratory biofeedback training system integrates PPG and IMU signals to extract cardiac and respiratory parameters, feeding them into an adaptive module that dynamically adjusts breathing guidance rates (GR) based on HRV levels and breathing alignment, providing real-time feedback to optimize cardio-respiratory coupling. The feedback and guidance cues are implemented in the form of a lotus-based design with the lotus flower corresponding to HRV and lotus leaf acting as the breathing guidance. The flower opening means high HRV and the flower closing means low HRV. The leaf opening guides the user to inhale and the leaf closing guides the user to exhale. The RF in RF Biofeedback Training and RF detection stands for Resonant Frequency.

between-subject experiment, allowing us to examine both the overall system performance and the effect of each design factor independently.[2]

5.1 Participants

The study sample comprised 48 participants (25 females, 23 males), aged 17 to 50 years (M = 22.98, SD = 5.11). Participants were recruited via word-of-mouth and snowball sampling. All participants reported normal or corrected-to-normal vision and no history of cardiovascular or respiratory illness. To control for potential confounding factors, they were instructed to refrain from consuming caffeine within 24 hours prior to the experiment.

5.2 Study Design and Procedure

Study Design. The goal of this study is to evaluate the effectiveness and user experience of our adaptive cardio-respiratory biofeedback system, and to understand how each of its core components contributes to overall performance. Specifically, we examine three design factors: **the hand-on-abdomen posture that enables embodied respiration sensing, the lotus-based visualization that delivers coordinated respiratory and HRV feedback, and the dual-factor adaptive feedback mechanism.** Given the functional interdependence of the components—respiration-driven adaptation requires the posture, and the lotus interface is necessary to simultaneously present HRV biofeedback and dual-factor breathing guidance—we adopt an incremental ablation design, adding one component at a time across conditions. This approach ensures that every condition represents a valid, fully operational version of the system, while allowing us to quantify the marginal contribution of each factor. Based on this design, we constructed a four-condition between-subject experiment, progressing from a minimal baseline to the fully integrated adaptive system, as shown in Figure 7.

Device Setup. As described in previous section, the smart ring provided higher signal quality than the smartwatch. Therefore, in this study we used the smart ring together with the mobile application. However, in the Baseline and Fixed conditions, the ring alone

[2]The study protocol was reviewed and approved by the university ethics review board. The compensation was consistent with the average earning of workers in the community where the study took place.

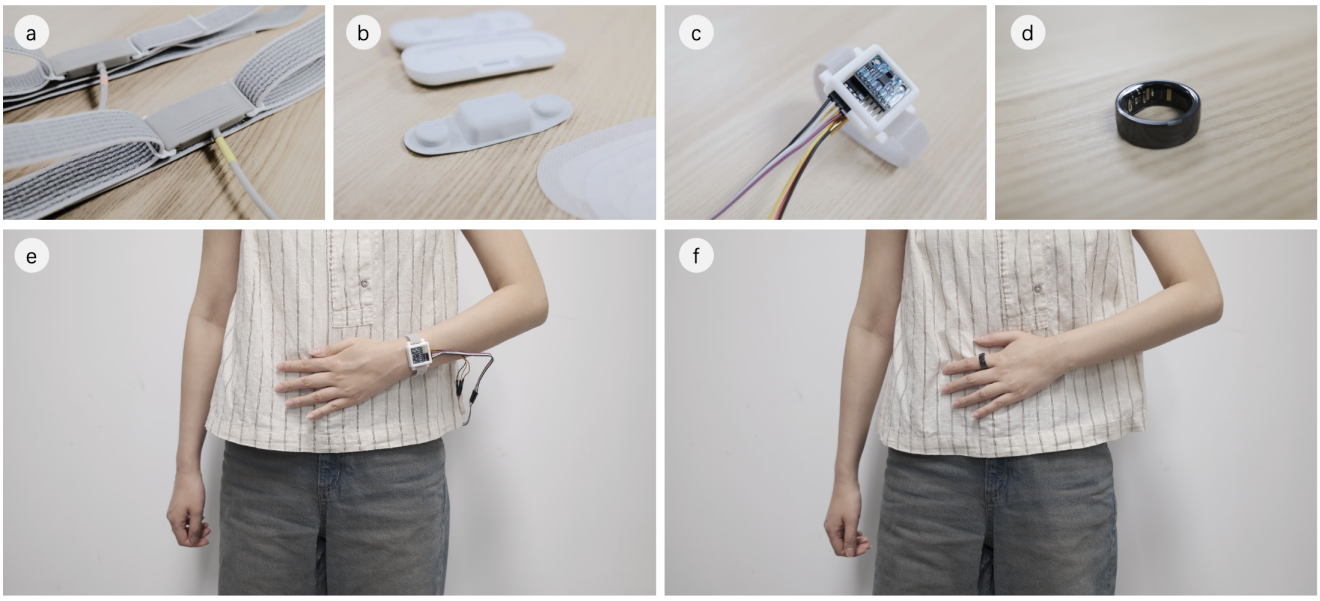

Figure 6: Experimental setup for signal quality assessment: (a) HKH-11C piezoelectric respiratory belt (reference device), (b) VIVALINK ECG patch (reference device), (c) smart watch device equipped with IMU and PPG sensors, and (d) smart ring with IMU and PPG sensors. (e) Smart ring signal quality assessment setup. (f) Smart watch signal quality assessment setup. For the setups in (e) and (f) The ECG patch and the respiratory belt are worn close to the body underneath the clothing.

could not reliably capture users' respiration signals, and we aimed to analyze the alignment between users' actual breathing and the guided breathing pattern. To address this, participants additionally wore an HKH-11C piezoelectric respiratory belt, and we synchronized the two devices using a brief motion-based impulse before analysis.

Study Procedure. Before the study began, participants were fitted with the devices, after which the ring recording was started and a 45-second baseline HRV measure was collected. We then induced stress using a standard TSST protocol [4]. To ensure a comparable level of stress across participants, the stress induction phase ended once a participant's HRV dropped to 85% of their personal baseline, at which point they proceeded to the next stage. Participants were randomly assigned to one of the four between-subject conditions. Each participant completed a 5-minute guided breathing session, using the system configuration corresponding to their assigned condition (Baseline, Fixed, Embodied-Fixed, or Embodied-Adaptive). During the breathing session, both the smart ring and the respiratory belt continuously recorded physiological signals. After completing the 5-minute session, participants evaluated their **experience with the entire biofeedback system (including the whole system of user interface, visualization, interaction flow, and physical comfort of the devices; excluding the prior TSST phase)**. They completed the User Engagement Scale – Short Form (UES-SF), NASA Task Load Index (NASA-TLX), System Usability and Credibility (SUS) and Credibility and Expectancy Questionnaire (CEQ). The rationale for selecting these measures is detailed in the following paragraphs.

5.3 Evaluation Metrics

We categorized our evaluation metrics into two main groups:

Physiological outcome measures: Objective indicators of the biofeedback training effect, primarily HRV changes. We recorded the trend of HRV throughout the training session, specifically measuring:

- **ΔHRV time series**: The averaged HRV trajectory over time for each condition, providing a direct representation of the system's physiological response profile.
- **HRV rise**: The magnitude of HRV (RMSSD) increase, reflecting immediate training effectiveness.
- **Duration above 120% of initial HRV**: The proportion of time during which HRV remained above 120% of its initial value, representing sustained physiological engagement.
- **Time to reach initial HRV + 15**: The latency from the beginning of training to the point where HRV increases by 15 ms. This metric captures how quickly participants enter a physiologically engaged state.
- **Breathing Alignment**: The percentage of time during which the participant's actual respiratory rate matched the guidance rate within specified tolerance bands (≥95%, 90–95%, 80–90%, <80%). Alignment is calculated as the ratio of the smaller to the larger of the two rates. The thresholds were selected based on typical respiratory rate measurement variability: ≥95% represents near-perfect synchronization within approximately 1.5× the sensor noise band; 90–95% indicates high alignment within 3× the noise band, reflecting minor but acceptable deviations; 80–90% reflects moderate alignment where participants generally follow the guidance

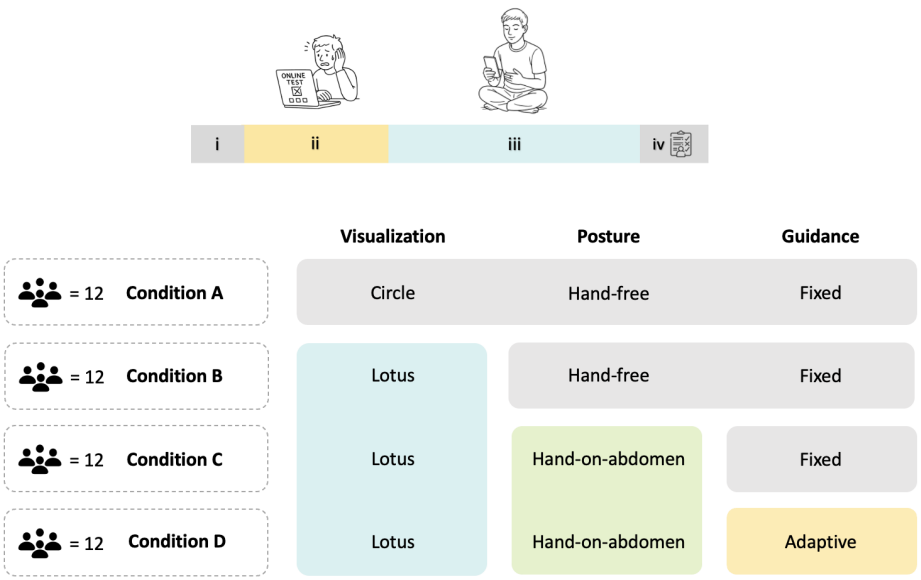

Figure 7: Procedure of User Study: (i) HRV baseline measurement; (ii) stress induction using the TSST protocol; (iii) 5-minute guided breathing session under the assigned condition; (iv) completion of post-session questionnaires (UES-SF, NASA-TLX, SUS, CEQ). Overview of the between-subject user study design and procedure (N=48). Participants were randomly assigned to one of four conditions (12 per condition), varying in Visualization (Circle vs. Lotus), Posture (Hand-free vs. Hand-on-abdomen), and Guidance type (Fixed vs. Adaptive).

rhythm but with noticeable timing differences; and <80% suggests difficulty maintaining the guided breathing pace.

User experience measures: Subjective measures reflecting participants' engagement, usability, and perceived workload, including:

- **User Experience**: Assessed using the **User Engagement Scale–Short Form (UES-SF)** [60], a validated instrument that captures four dimensions of engagement: focused attention, perceived usability, aesthetic appeal, and reward. We selected the UES-SF because its four dimensions closely correspond to the cognitive and experiential demands of our system. We sought to evaluate whether the added design elements effectively attract users' **focused attention** or introduce distraction, and whether the additional software and hardware components negatively affect **perceived usability**. Given our distinctive visualization design, we were also interested in users' aesthetic responses, captured by **aesthetic appeal**. Finally, we assessed whether these features collectively enhance users' subjective sense of benefit, reflected in **reward**. These dimensions together make UES-SF well aligned with the interaction characteristics of our breathing tasks.
- **Perceived Workload**: Measured by the **NASA Task Load Index (NASA-TLX)** [35], a widely used instrument evaluating subjective workload across six dimensions (mental, physical, temporal demand, performance, effort, and frustration). We included NASA-TLX to assess whether the embodied posture, additional sensing hardware, and adaptive interaction introduce unintended cognitive or physical burden. Unlike engagement measures, NASA-TLX allows us to quantify potential costs of using the system—ensuring that performance gains from adaptivity do not come at the expense of increased workload.
- **System Usability and Credibility**: Assessed using the **System Usability Scale (SUS)** [49] and the **Credibility and Expectancy Questionnaire (CEQ)** [25]. The SUS evaluates overall usability, including perceived ease of use and learnability. The CEQ measures participants' perceived credibility of the system and expectations of its effectiveness. We adopted SUS to evaluate whether participants found the system intuitive and easy to operate, given that our interface integrates novel visualization and feedback components. In addition, the CEQ was included because biofeedback efficacy strongly depends on users' trust in the underlying physiological mechanisms. Since our system adapts pacing based on personal HRV and respiration signals, measuring participants' perceived credibility and expectancy is essential to understanding whether users view the adaptive strategy as legitimate and effective.

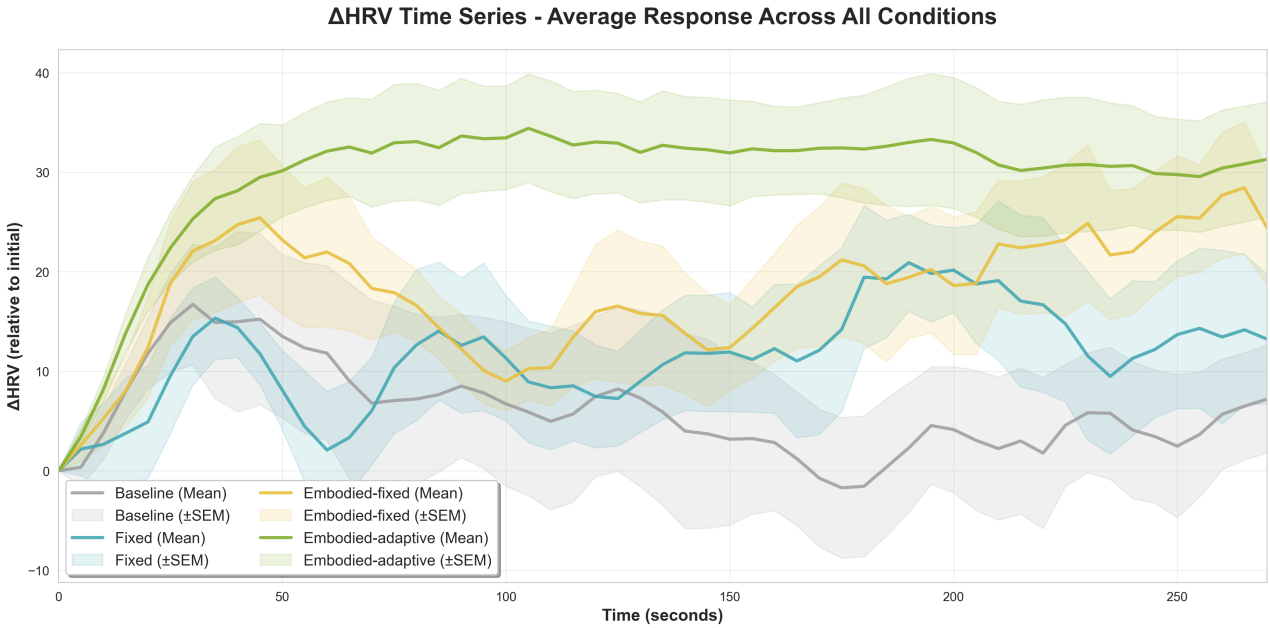

Figure 8: Overall HRV response across all participants.

5.4 Results

5.4.1 HRV Response. From the HRV time series (Figure 8), we observe that the Fixed and Baseline groups show minimal differences, with the Fixed group exhibiting slightly higher HRV only toward the later part of the session. In contrast, both embodied conditions demonstrate a faster and larger HRV increase at the beginning of training compared to the non-embodied conditions. Throughout the entire session, the Adaptive group maintains substantially more stable HRV trajectories than all other groups. Meanwhile, all three intervention methods (Fixed, Embodied-fixed, and Embodied-adaptive) outperformed the Baseline condition in terms of **peak HRV**. For the **HRV rise from initial to training end**, the Embodied-adaptive condition showed a notable increase (M = 30.2, SD = 20.6) compared to Baseline (M = 3.4, SD = 30.3), with a mean difference of 26.8 ms (p = 0.021). The **total duration** during which HRV remained above 120% of the initial value was longest under Embodied-adaptive guidance (M = 263.3 s, SD = 74.5), which was **47.3% higher** than Fixed guidance and **76.6% higher** than Baseline (M = 149.1 s, SD = 127.6; p = 0.015).

5.4.2 Breathing Alignment. Breathing alignment was substantially higher in embodied conditions, shown in Figure 9. The **Embodied-adaptive** condition achieved the best alignment, with **82%** of training time at ≥80% alignment and **36%** at ≥95%, indicating near-perfect synchronization with the dynamically adjusted guidance. **Embodied-fixed** showed similarly strong results (**79%** at ≥80%, **27%** at ≥95%).

In contrast, the **Fixed** condition exhibited the poorest alignment, with only **50%** of time at ≥80% and **50%** below the acceptable threshold. The **Baseline** condition fell in between (**61%** at ≥80%).

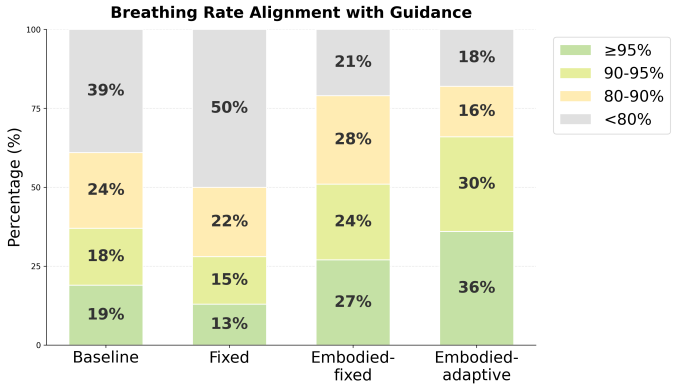

Figure 9: Distribution of Breathing Pacing Adherence. A comparison of participants' breathing synchronization accuracy across the four experimental conditions. The stacked bars illustrate the percentage of session time spent in four distinct adherence tiers: High (≥95%), Good (90–95%), Moderate (80–90%), and Low (<80%). Among the four conditions, the Embodied-adaptive condition achieved the best alignment. Among the three factors, the addition of the Embodied posture allowed for the strongest breathing adherence results.

5.4.3 User Experience. The **Aesthetic Appeal** dimension of UES-SF showed significant differences across conditions. All three intervention methods (Fixed, Embodied-fixed, and Embodied-adaptive) received higher aesthetic ratings than Baseline (Baseline vs. Fixed: $p = 0.025$; Baseline vs. Embodied-fixed: $p = 0.008$; Baseline vs. Embodied-adaptive: $p = 0.006$). Other UES dimensions—Focused

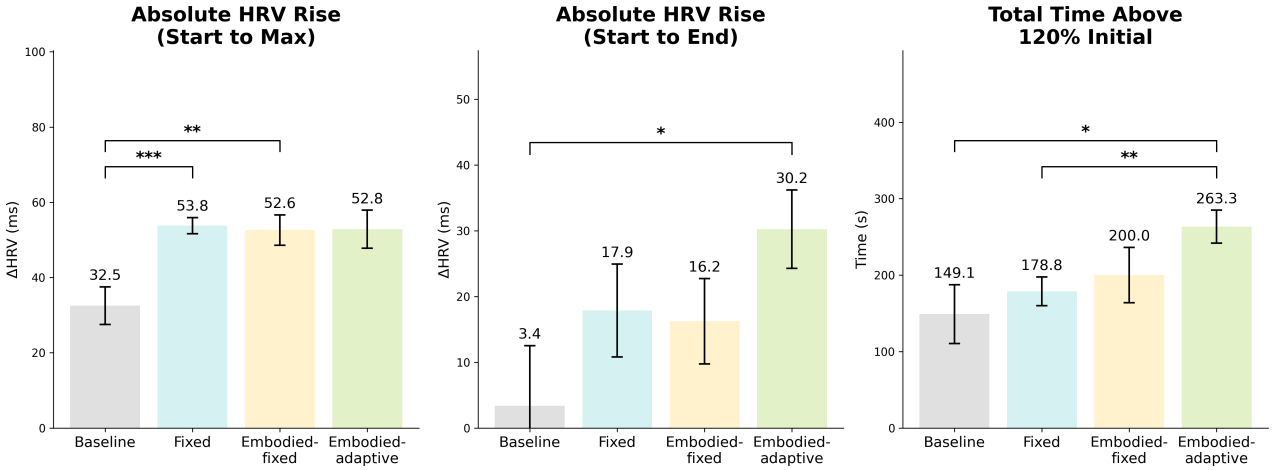

Figure 10: Comparison of HRV metrics across four conditions. Bars represent the mean values with error bars indicating the standard error of the mean (SEM). Asterisks denote statistically significant differences between pairs of conditions based on independent-samples t-tests ($^{*}p < 0.05$, $^{**}p < 0.01$, $^{***}p < 0.001$). The Lotus UI and the adaptive strategy both increase HRV rise. All three factors contribute to maintaining a more desirable physiological state and enabling users to reach this state more quickly.

Attention, Perceived Usability, and Reward—did not show significant differences between conditions, indicating that these added factors did not impair users' focused attention or usability.

5.4.4 Perceived Workload. The NASA-TLX results revealed that the **Fixed** condition consistently produced the highest workload scores across multiple dimensions. Specifically, Fixed guidance was associated with significantly higher **Mental Demand** compared to Baseline and Embodied-adaptive conditions, and significantly higher **Physical Demand** compared to Embodied-adaptive. The **Performance** dimension (self-assessed task success, reverse-scored) was significantly worse under Fixed guidance compared to both Embodied conditions. **Frustration** was also significantly higher for Fixed compared to Baseline. No significant differences were observed for Temporal Demand across conditions. These results indicate that the three added components—the lotus visualization, the embodied hand-on-abdomen posture, and the adaptive pacing mechanism—did not introduce additional cognitive burden.

5.4.5 System Usability and Credibility. All four conditions showed comparable scores on the **System Usability Scale (SUS)**, with mean scores ranging from 5.40 to 5.52 (out of 7), indicating that the different guidance modalities did not negatively impact perceived usability. Similarly, the **CEQ** (Credibility and Expectancy) questionnaire showed no significant differences between conditions, suggesting that participants perceived all methods as similarly credible for achieving relaxation outcomes.

5.4.6 Overall Preference. Participants' post-experiment rankings indicated a strong preference for the Embodied-adaptive condition, shown in Figure 12. It was selected as the top choice (Rank 1) by 60% of participants, with only 8% rating it as the least preferred. Conversely, the Baseline condition was rated as the worst (Rank 4) by 62% of participants. The intermediate conditions showed a preference for the embodied posture; the Embodied-fixed condition received a substantial number of Rank 2 ratings (33%), whereas the Fixed condition was most frequently placed in Rank 3 (44%).

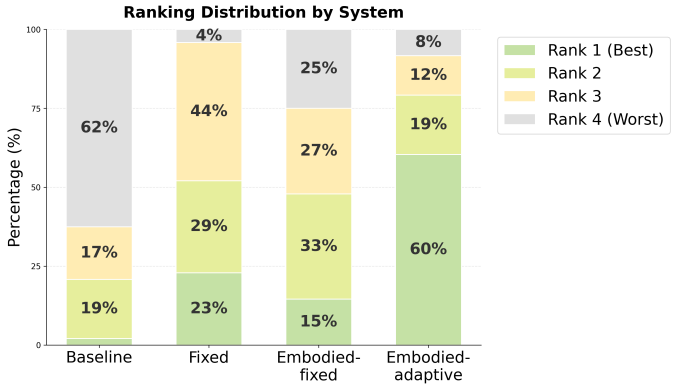

Figure 12: Distribution of participant preference rankings across four conditions. Participants ranked each experimental condition from 1 (Best) to 4 (Worst) upon completion of the study. The stacked bar chart illustrates that the Embodied-adaptive condition was the most preferred, with 60% of participants ranking it as their top choice (Rank 1). Conversely, the Baseline condition was the least preferred, designated as Rank 4 (Worst) by 62% of participants. The Fixed and Embodied-fixed conditions occupied the intermediate preference tiers, with mixed rankings primarily distributed between Rank 2 and Rank 3.

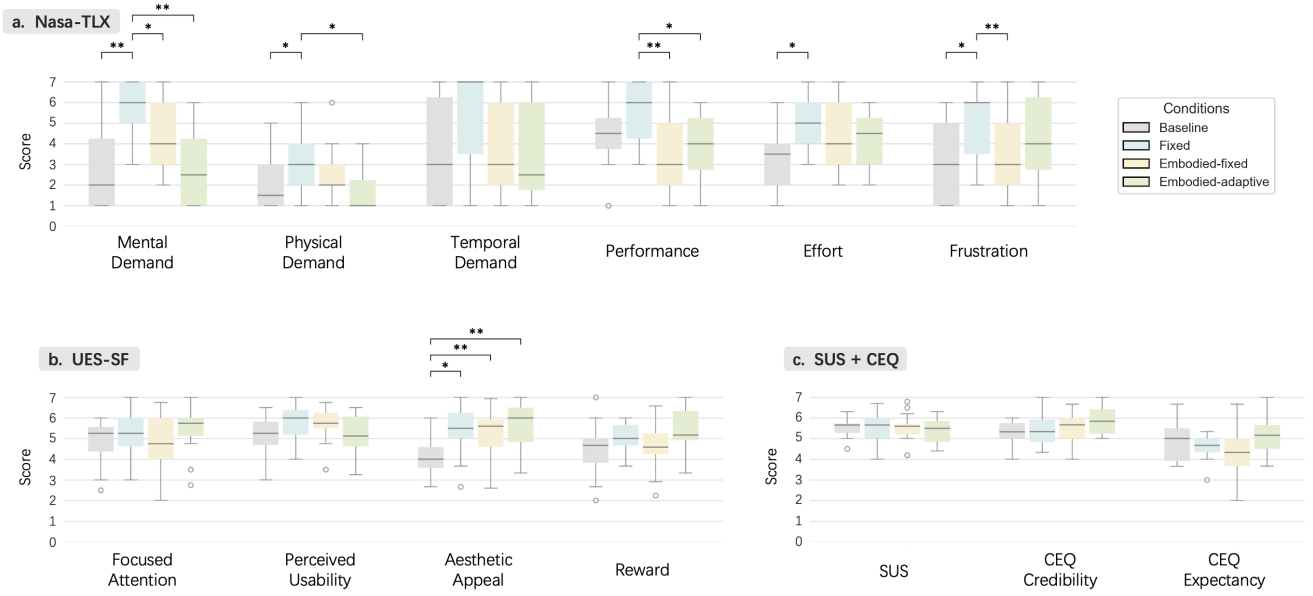

Figure 11: Comparison of subjective evaluation metrics across four experimental conditions. (a) NASA-TLX results indicate that the Fixed condition imposed significantly higher workload, specifically in Mental Demand, Performance (perceived failure), and Frustration, compared to the Embodied-adaptive condition (*p < 0.05). (b) UES-SF results highlight that regarding Aesthetic Appeal, all three visual intervention conditions (Fixed, Embodied-fixed, Embodied-adaptive) were rated significantly higher than the Baseline (p < 0.01 for Embodied conditions). (c) SUS and CEQ results show no statistically significant differences, suggesting comparable perceived usability and credibility across the intervention designs. Box plots represent the median and interquartile range (IQR), with whiskers extending to 1.5 × IQR. Asterisks indicate statistically significant differences between conditions based on the Mann-Whitney U test (*p < 0.05, **p < 0.01, ***p < 0.001).**

5.5 Findings

We organized the results according to specific outcome dimensions: Drawing from the results, we synthesized the contribution of each factor to the biofeedback training outcomes.

5.5.1 Visual Design of the Lotus: Enhanced Affect but Increased Workload. Comparing the Fixed and Baseline groups, introducing the Lotus visualization improved HRV rise—particularly in the later stages of training—and received high aesthetic ratings, with many participants expressing strong preference for the design during interviews. However, because the interface differs from conventional breathing guides, it imposed additional mental workload and may have contributed to reduced alignment with the breathing guidance.

5.5.2 Embodied Interaction Posture: Enhanced Respiratory Alignment and Faster Physiological Engagement. Both embodied conditions exhibited a noticeably faster and larger initial HRV increase compared to the non-embodied conditions, indicating that the posture helped participants enter a physiologically engaged state more rapidly. Embodied posture also yielded markedly better breathing alignment: both Embodied-fixed and Embodied-adaptive achieved higher proportions of time at strong alignment levels (≥80% and ≥95%) compared to Baseline and Fixed. This suggests that placing the hand on the abdomen reinforced participants' perception of their breathing rhythm and depth, enabling more consistent synchronization with the guided rate. Overall, these results highlight that the embodied interaction posture serves as an effective mechanism for grounding users in their bodily sensations, facilitating more stable entrainment and amplifying the benefits of both fixed and adaptive guidance.

5.5.3 Adaptive Strategy: Improved Stability, Sustained Engagement, and Superior Entrainment. The adaptive pacing strategy consistently outperformed all other conditions across both physiological and behavioral measures. It enabled participants to enter a regulated state more quickly while also producing more sustained training effects. Participants in the Embodied-adaptive condition demonstrated the most stable HRV trajectories throughout the session, with substantially reduced fluctuations compared to both fixed and non-embodied groups, indicating that adjusting the breathing rate in real time helps users maintain a more stable and manageable physiological state. Adaptive pacing also achieved the highest breathing alignment among all groups: participants maintained

≥80% alignment for 82% of the session and ≥95% alignment for 36% of the session, reflecting near-perfect synchronization with the guided rhythm. Although the adaptive method introduces the most interaction requirements (including a more complex UI, posture maintenance, and a dynamic guidance mechanism), its overall workload scores were nonetheless lower than those of the Fixed and Embodied-fixed groups, and not significantly different from Baseline. This suggests that the improved breathing experience afforded by adaptivity allowed participants to relax more effectively, thereby reducing their perceived workload.

5.5.4 System-Level Effectiveness: Combined Impact of All Components. Across all outcome measures, the fully integrated Embodied-adaptive condition consistently produced the strongest performance. It yielded the largest HRV gains, the highest levels of breathing alignment, and the lowest perceived workload among the four conditions. These results indicate that visual guidance, embodied interaction, and adaptive pacing collectively contribute to improved cardio-respiratory training outcomes when used together. While each component offers measurable benefits on its own, their combined use produced the most robust physiological and experiential improvements observed in the study.

6 Discussion

6.1 Feel Your Signals: Integrating Embodied Interaction and Wearable Physiological Sensing

The first loop in this system is the inner loop of action and cognition. Human actions are shaped by cognition, while actions in turn influence cognition. According to embodied cognition theory, off-line cognition is grounded in the body [76]. Just as biofeedback makes physiological signals visible to enhance consciousness and self-regulation, direct bodily perception can also strengthen awareness and support better control over one's physiological state. In the design rationale section, we demonstrated this through hand placement, which amplified diaphragmatic breathing by enhancing awareness via embodied interaction.

In our system design, we extend this principle by **integrating embodied interaction with physiological sensing through a hand-worn device**. This integration illustrates that whenever embodied interaction engages a specific part of the body, wearable devices can function as bodily extensions to capture additional dimensions of physiological signals and deliver feedback. Such feedback, combined with the heightened bodily awareness fostered by embodied interaction, jointly shapes users' cognition of their current state. This cognitive shift, in turn, influences their physiological conditions and subsequent behaviors.

6.2 Designing for Synergy: How Multimodal Components Work Together to Enhance Biofeedback

Our findings show that the three core design components—visual feedback, embodied interaction, and adaptive pacing—each contribute distinct yet complementary benefits that collectively strengthen the effectiveness of cardio-respiratory biofeedback. The Lotus visualization enhances affective experience and supports long-term HRV improvement; the embodied posture deepens respiratory awareness and improves entrainment; and the adaptive mechanism stabilizes physiological responses and sustains engagement by dynamically aligning guidance with users' moment-to-moment states. Importantly, these components do not merely add independent advantages—they interact synergistically. The fully integrated Embodied-Adaptive condition yielded the highest HRV gains, the strongest breathing alignment, and the lowest perceived workload, demonstrating that combining multimodal cues, bodily engagement, and real-time physiological adaptation creates a more robust and user-centered biofeedback experience. This synergy validates our system design rationale and highlights the importance of approaching biofeedback as an integrated interaction ecology rather than a single-modality intervention.

6.3 More Insights, Not More Devices: Lowering the Barrier to Pervasive Health Monitoring

Modern health monitoring technologies are evolving in two main directions: toward more accurate sensing methods and toward more accessible deployment in everyday health management applications. Wearable devices primarily enable the latter. While dedicated devices have supported biofeedback, real accessibility comes from wearable devices already embedded in people's routines. This is why we chose to bring our system onto general-purpose wearable devices. Smart rings and smart watches exemplify viable platforms, and our signal quality assessments confirm that any device integrating both IMU and PPG sensors can support the same functionalities.

In this study, we prioritized IMU-based respiration detection due to its superior accuracy over PPG. However, our evaluations also demonstrated that respiration can be reliably derived from PPG alone. Notably, our method repurposes motion artifacts—typically considered noise—as a novel signal source for respiration detection. Combined with heart rate data obtained via PPG, **this enables cardio-respiratory biofeedback training even on devices equipped solely with PPG sensors**. Reducing sensor requirements while maintaining functionality is central to our vision of democratizing biofeedback for real-world, everyday use.

6.4 Limitations

This work has several limitations that also point to promising directions for future research. First, our evaluation focused on short-term effects measured immediately after system use. While these findings demonstrate the feasibility and immediate impact of the system, they do not provide evidence regarding its long-term efficacy. Future studies should therefore incorporate longitudinal designs to assess sustained benefits over extended periods of practice. Second, in the user study, we conducted user experiments only with the smart ring. Although this choice highlights the potential of emerging wearable form factors, it leaves open the question of whether similar effects can be replicated with the smart watch-based implementation. Extending the evaluation to include smart watch users, and eventually translating the system to smartphones—the most ubiquitous personal devices—would greatly enhance accessibility and generalizability. Third, the current adaptive biofeedback design

primarily relies on motion-based respiration monitoring, which can capture breathing rate but only indirectly reflects depth. Our results suggest that respiration depth can also be reliably estimated from motion signals. Leveraging this indicator as an additional feedback channel could enable more fine-grained adaptive control, allowing the system to dynamically tailor both breathing frequency and depth to optimize training outcomes.

7 Conclusion

This work presents a novel approach to **dual-factor cardio-respiratory biofeedback** through a **hand-worn device**, integrated with an **embodied interaction paradigm**. We demonstrated that a wearable system dynamically adapting to both cardiac and respiratory signals can significantly enhance physiological outcomes, while a simple, intentional posture like hand-on-abdomen serves to both deepen the user's mind-body connection and improve signal quality. Together, these contributions create a more effective, engaging, and ecologically valid pathway for personalized biofeedback, enabling better accessibility for users in their everyday environments.

Acknowledgments

This work is supported by National Key R&D Program of China under Grant No. 2024YFB2808800 & 2024YFB2808803.

References

[1] S Akselrod, D Gordon, F A Ubel, D C Shannon, A C Berger, and R J Cohen. 1981. Power spectrum analysis of heart rate fluctuation: a quantitative probe of beat-to-beat cardiovascular control. *Science* 213, 4504 (July 1981), 220–222.

[2] Mohamed Ali, Ali Elsayed, Arnaldo Mendez, Yvon Savaria, and Mohamad Sawan. 2021. Contact and Remote Breathing Rate Monitoring Techniques: A Review. *IEEE Sensors Journal* 21, 13 (2021), 14569–14586. doi:10.1109/JSEN.2021.3072607

[3] John Allen. 2007. Photoplethysmography and its application in clinical physiological measurement. *Physiological Measurement* 28 (04 2007), R1–39. doi:10.1088/0967-3334/28/3/R01

[4] Mohammed A Almazrouei, Ruth M Morgan, and Itiel E Dror. 2023. A method to induce stress in human subjects in online research environments. *Behavior research methods* 55, 5 (2023), 2575–2582.

[5] Sara Alnasser, Dalal Alkalthem, Sara Alenazi, Muneera Alsowinea, Narin Alanazi, and Ahmed Al Fagih. 2023. The reliability of the Apple Watch's electrocardiogram. *Cureus* 15, 12 (Dec. 2023), e49786.

[6] Alessandra Angelucci and Andrea Aliverti. 2023. An IMU-based wearable system for respiratory rate estimation in static and dynamic conditions. *Cardiovasc. Eng. Technol.* 14, 3 (June 2023), 351–363.

[7] Sai Balaji, Nachum Plonka, Mike Atkinson, Malathy Muthu, Minvydas Ragulskis, Alfonsas Vainoras, and Rollin McCraty. 2025. Heart rate variability biofeedback in a global study of the most common coherence frequencies and the impact of emotional states. *Sci. Rep.* 15, 1 (Jan. 2025), 3241.

[8] Carla Barreiros, Eduardo Veas, and Viktoria Pammer. 2018. Bringing Nature into Our Lives: Using Biophilic Design and Calm Computing Principles to Improve Well-Being and Performance. In *International Conference on Human-Computer Interaction*. Springer, 99–109.

[9] G G Berntson, J T Bigger, Jr, D L Eckberg, P Grossman, P G Kaufmann, M Malik, H N Nagaraja, S W Porges, J P Saul, P H Stone, and M W van der Molen. 1997. Heart rate variability: origins, methods, and interpretive caveats. *Psychophysiology* 34, 6 (Nov. 1997), 623–648.

[10] G G Berntson, J T Cacioppo, and K S Quigley. 1993. Respiratory sinus arrhythmia: autonomic origins, physiological mechanisms, and psychophysiological implications. *Psychophysiology* 30, 2 (March 1993), 183–196.

[11] BioSign GmbH. 2010. BioSign Qiu. https://site.biosign.de/en-gb/qiu. Accessed: September 12, 2025.

[12] S. Blok, M.A. Piek, I.I. Tulevski, G.A. Somsen, and M.M. Winter. 2021. The accuracy of heartbeat detection using photoplethysmography technology in cardiac patients. *Journal of Electrocardiology* 67 (2021), 148–157. doi:10.1016/j.jelectrocard.2021.06.009

[13] Johannes Blum, Christoph Rockstroh, and Anja S Göritz. 2019. Heart rate variability biofeedback based on slow-paced breathing with immersive virtual reality nature scenery. *Front. Psychol.* 10 (Sept. 2019), 2172.

[14] Josh Border, Andrew Lefevre, Vishal Jain, and Alain Nogaret. 2025. Cardiorespiratory coupling improves cardiac pumping efficiency in heart failure. arXiv:2507.00597 [q-bio.TO] https://arxiv.org/abs/2507.00597

[15] Ekaterina I Borovkova, Mikhail D Prokhorov, Anton R Kiselev, Aleksey N Hramkov, Sergey A Mironov, Mikhail V Agaltsov, Vladimir I Ponomarenko, Anatoly S Karavaev, Oksana M Drapkina, and Thomas Penzel. 2022. Directional couplings between the respiration and parasympathetic control of the heart rate during sleep and wakefulness in healthy subjects at different ages. *Front. Netw. Physiol.* 2 (Sept. 2022), 942700.

[16] Lluis Capdevila, Eva Parrado, Juan Ramos-Castro, Rafael Zapata-Lamana, and Jaume F Lalanza. 2021. Resonance frequency is not always stable over time and could be related to the inter-beat interval. *Sci. Rep.* 11, 1 (April 2021), 8400.

[17] Denisse Castaneda, Aibhlin Esparza, Mohammad Ghamari, Cinna Soltanpur, and Homer Nazeran. 2018. A review on wearable photoplethysmography sensors and their potential future applications in health care. *Int. J. Biosens. Bioelectron.* 4, 4 (Aug. 2018), 195–202.

[18] Paolo Castiglioni, Andrea Faini, Gianfranco Parati, and Marco Di Rienzo. 2007. Wearable Seismocardiography. In *2007 29th Annual International Conference of the IEEE Engineering in Medicine and Biology Society* (Lyon, France). IEEE.

[19] Vivek Chandel, Arijit Sinharay, Nasimuddin Ahmed, and Avik Ghose. 2016. Exploiting IMU Sensors for IOT Enabled Health Monitoring. 21–22. doi:10.1145/2933566.2933569

[20] Nan Chao, Wei Huang, and Xingjun Wang. 2023. Design of a respiratory biofeedback serious game for stress management based on HRV analysis. In *Communications in Computer and Information Science*. Springer Nature Switzerland, Cham, 16–24.

[21] Qi Chen, Jiachen Du, Zhihao Yao, Yuanling Feng, Guanhong Liu, Ning Ni, Zhenyu Wu, Haoran Liu, Xijing Chen, and Haipeng Mi. 2025. Breath of life: A biofeedback game with diverse breathing techniques for enhanced real-life emotion regulation. In *Proceedings of the Extended Abstracts of the CHI Conference on Human Factors in Computing Systems* (Yokohama Japan). ACM, New York, NY, USA, 1–9.

[22] Luca Chittaro, Marta Serafini, and Yvonne Vulcano. 2024. Virtual reality experiences for breathing and relaxation training: The effects of real vs. placebo biofeedback. *Int. J. Hum. Comput. Stud.* 188, 103275 (Aug. 2024), 103275.

[23] Michael Chu, Thao Nguyen, Vaibhav Pandey, Yongxiao Zhou, Hoang N Pham, Ronen Bar-Yoseph, Shlomit Radom-Aizik, Ramesh Jain, Dan M Cooper, and Michelle Khine. 2019. Respiration rate and volume measurements using wearable strain sensors. *NPJ Digit. Med.* 2, 1 (Feb. 2019), 8.

[24] Fengzhen Cui, Yuntao Wang, Shenshen Lei, and Yuanchun Shi. 2024. CardboardHRV: Bridging virtual reality and biofeedback with a cost-effective heart rate variability system. In *Extended Abstracts of the CHI Conference on Human Factors in Computing Systems* (Honolulu HI USA). ACM, New York, NY, USA, 1–6.

[25] Grant J Devilly and Thomas D Borkovec. 2000. Psychometric properties of the credibility/expectancy questionnaire. *Journal of behavior therapy and experimental psychiatry* 31, 2 (2000), 73–86.

[26] Thomas E Dick, David M Baekey, Julian F R Paton, Bruce G Lindsey, and Kendall F Morris. 2009. Cardio-respiratory coupling depends on the pons. *Respir. Physiol. Neurobiol.* 168, 1-2 (Aug. 2009), 76–85.

[27] Thomas E Dick, Yee-Hsee Hsieh, Rishi R Dhingra, David M Baekey, Roberto F Galán, Erica Wehrwein, and Kendall F Morris. 2014. Cardiorespiratory coupling: common rhythms in cardiac, sympathetic, and respiratory activities. *Progress in brain research* 209 (2014), 191–205.

[28] Filipa Esgalhado, Arnaldo Batista, Valentina Vassilenko, Sara Russo, and Manuel Ortigueira. 2022. Peak Detection and HRV Feature Evaluation on ECG and PPG Signals. *Symmetry* 14, 6 (2022). doi:10.3390/sym14061139

[29] Alfredo J Garcia, 3rd, Jenna E Koschnitzky, Tatiana Dashevskiy, and Jan-Marino Ramirez. 2013. Cardiorespiratory coupling in health and disease. *Auton. Neurosci.* 175, 1-2 (April 2013), 26–37.

[30] A. Gaucher, D. Frasca, O. Mimoz, and B. Debaene. 2012. Accuracy of respiratory rate monitoring by capnometry using the Capnomask® in extubated patients receiving supplemental oxygen after surgery. *British Journal of Anaesthesia* 108, 2 (2012), 316–320. doi:10.1093/bja/aer383

[31] Amy L Gentzler, Aimee K Santucci, Maria Kovacs, and Nathan A Fox. 2009. Respiratory sinus arrhythmia reactivity predicts emotion regulation and depressive symptoms in at-risk and control children. *Biol. Psychol.* 82, 2 (Oct. 2009), 156–163.

[32] Oonagh M Giggins, Ulrik Mccarthy Persson, and Brian Caulfield. 2013. Biofeedback in rehabilitation. *J. Neuroeng. Rehabil.* 10, 1 (June 2013), 60.

[33] Hyonyoung Han and Jung Kim. 2012. Artifacts in wearable photoplethysmographs during daily life motions and their reduction with least mean square based active noise cancellation method. *Computers in Biology and Medicine* 42, 4 (2012), 387–393. doi:10.1016/j.compbiomed.2011.12.005

[34] Tian Hao, Chongguang Bi, Guoliang Xing, Roxane Chan, and Linlin Tu. 2017. MindfulWatch. *Proc. ACM Interact. Mob. Wearable Ubiquitous Technol.* 1, 3 (Sept. 2017), 1–19.

[35] Sandra G Hart and Lowell E Staveland. 1988. Development of NASA-TLX (Task Load Index): Results of empirical and theoretical research. In *Advances in psychology*. Vol. 52. Elsevier, 139–183.

[36] Javier Hernandez, Daniel McDuff, and Rosalind W. Picard. 2015. Biowatch: Estimation of heart and breathing rates from wrist motions. In *2015 9th International Conference on Pervasive Computing Technologies for Healthcare (PervasiveHealth)*. 169–176. doi:10.4108/icst.pervasivehealth.2015.259064

[37] LaBarron Hill and Anne Siebenbrock. 2009. All are measures created equal? Heart rate variability and respiration. Biomed Sci Instrum, 45, 71-76. *Biomedical sciences instrumentation* 45 (02 2009), 71–6.

[38] Yu-Chen Huang, Ting-Yu Lin, Hau-Tieng Wu, Po-Jui Chang, Chun-Yu Lo, Tsai-Yu Wang, Chih-Hsi Scott Kuo, Shu-Min Lin, Fu-Tsai Chung, Horng-Chyuan Lin, Meng-Heng Hsieh, and Yu-Lun Lo. 2021. Cardiorespiratory coupling is associated with exercise capacity in patients with chronic obstructive pulmonary disease. *BMC Pulm. Med.* 21, 1 (Jan. 2021), 22.

[39] Daniel E Hurtado, Angel Abusleme, and Javier A P Chávez. 2020. Non-invasive continuous respiratory monitoring using temperature-based sensors. *J. Clin. Monit. Comput.* 34, 2 (April 2020), 223–231.

[40] Preeti Jagadev and Lalat Indu Giri. 2020. Non-contact monitoring of human respiration using infrared thermography and machine learning. *Infrared Phys. Technol.* 104, 103117 (Jan. 2020), 103117.

[41] Rene Jaros, Jiri Koutny, Martina Ladrova, and Radek Martinek. 2023. Novel phonocardiography system for heartbeat detection from various locations. *Sci. Rep.* 13, 1 (Sept. 2023), 14392.

[42] Harim Jeong, Joo Hun Yoo, Michelle Goh, and Hayeon Song. 2024. Deep breathing in your hands: designing and assessing a DTx mobile app. *Front. Digit. Health* 6 (Jan. 2024), 1287340.

[43] Shinya Kano, Nutpaphat Jarulertwathana, Syazwani Mohd-Noor, Jerome K. Hyun, Ryota Asahara, and Harutaka Mekaru. 2022. Respiratory Monitoring by Ultrafast Humidity Sensors with Nanomaterials: A Review. *Sensors* 22, 3 (2022). doi:10.3390/s22031251

[44] Heesoo Kim and Jinho Jeong. 2020. Non-Contact Measurement of Human Respiration and Heartbeat Using W-band Doppler Radar Sensor. *Sensors* 20, 18 (2020). doi:10.3390/s20185209

[45] Hye-Geum Kim, Eun-Jin Cheon, Dai-Seg Bai, Young Hwan Lee, and Bon-Hoon Koo. 2018. Stress and heart rate variability: A meta-analysis and review of the literature. *Psychiatry Investig.* 15, 3 (March 2018), 235–245.

[46] David Kirsh. 2013. Embodied cognition and the magical future of interaction design. *ACM Transactions on Computer-Human Interaction (TOCHI)* 20, 1 (2013), 1–30.

[47] Paul Lehrer, Karenjot Kaur, Agratta Sharma, Khushbu Shah, Robert Huseby, Jay Bhavsar, Phillip Sgobba, and Yingting Zhang. 2020. Heart rate variability biofeedback improves emotional and physical health and performance: A systematic review and meta analysis. *Appl. Psychophysiol. Biofeedback* 45, 3 (Sept. 2020), 109–129.

[48] Paul M Lehrer, Evgeny Vaschillo, and Bronya Vaschillo. 2000. Resonant frequency biofeedback training to increase cardiac variability: Rationale and manual for training. *Applied psychophysiology and biofeedback* 25, 3 (2000), 177–191.

[49] James R Lewis. 2018. The system usability scale: past, present, and future. *International Journal of Human–Computer Interaction* 34, 7 (2018), 577–590.

[50] Jinfeng Li, Yong Fan, Wenbin Shi, Mengwei Li, Lixuan Li, Wei Yan, Muyang Yan, Zhengbo Zhang, and Chien-Hung Yeh. 2024. Examining the practical importance of nonstationary cardio-respiratory coupling detection in breathing training: a methodological appraisal. *PeerJ* 12 (Nov. 2024), e18551.

[51] Rong-Hao Liang, Bin Yu, Mengru Xue, Jun Hu, and Loe MG Feijs. 2018. BioFidget: Biofeedback for respiration training using an augmented fidget spinner. In *Proceedings of the 2018 CHI conference on human factors in computing systems*. 1–12.

[52] Guiping Lin, Qiuling Xiang, Xiaodong Fu, Shuzhen Wang, Sheng Wang, Sijuan Chen, Li Shao, Yan Zhao, and Tinghuai Wang. 2012. Heart rate variability biofeedback decreases blood pressure in prehypertensive subjects by improving autonomic function and baroreflex. *J. Altern. Complement. Med.* 18, 2 (Feb. 2012), 143–152.

[53] Zhuofu Liu, Vincenzo Cascioli, and Peter W. McCarthy. 2023. Healthcare Monitoring Using Low-Cost Sensors to Supplement and Replace Human Sensation: Does It Have Potential to Increase Independent Living and Prevent Disease? *Sensors* 23, 4 (2023). doi:10.3390/s23042139

[54] Yanick Xavier Lukic, Chen-Hsuan Iris Shih, Alvaro Hernandez Reguera, Amanda Cotti, Elgar Fleisch, and Tobias Kowatsch. 2021. Physiological responses and user feedback on a gameful breathing training app: Within-subject experiment. *JMIR Serious Games* 9, 1 (Feb. 2021), e22802.

[55] Xiao Ma, Zi-Qi Yue, Zhu-Qing Gong, Hong Zhang, Nai-Yue Duan, Yu-Tong Shi, Gao-Xia Wei, and You-Fa Li. 2017. The Effect of Diaphragmatic Breathing on Attention, Negative Affect and Stress in Healthy Adults. *Frontiers in Psychology* Volume 8 - 2017 (2017). doi:10.3389/fpsyg.2017.00874

[56] Wolf E Mehling, Cynthia Price, Jennifer J Daubenmier, Mike Acree, Elizabeth Bartmess, and Anita Stewart. 2012. The multidimensional assessment of interoceptive awareness (MAIA). *PloS one* 7, 11 (2012), e48230.

[57] Dario Monzani, Ketti Mazzocco, and Gabriella Pravettoni. 2021. A meta-analysis on heart rate variability biofeedback and depressive symptoms. *Sci. Rep.* 11, 1 (March 2021), 6650.

[58] Margaret Morris and Farzin Guilak. 2009. Mobile heart health: project highlight. *IEEE Pervasive Computing* 8, 2 (2009), 57–61.

[59] Andrea Nicolò, Carlo Massaroni, Emiliano Schena, and Massimo Sacchetti. 2020. The importance of respiratory rate monitoring: From healthcare to sport and exercise. *Sensors (Basel)* 20, 21 (Nov. 2020), 6396.

[60] Heather L O'Brien, Paul Cairns, and Mark Hall. 2018. A practical approach to measuring user engagement with the refined user engagement scale (UES) and new UES short form. *International Journal of Human-Computer Studies* 112 (2018), 28–39.

[61] Vishnunarayan G Prabhu, Laura M Stanley, Courtney Linder, and Robert Morgan. 2020. Analyzing the efficacy of a restorative virtual reality environment using HRV biofeedback for pain and anxiety management. In *2020 IEEE international conference on human-machine systems (ICHMS)*. IEEE, 1–4.

[62] Christoph Rockstroh, Johannes Blum, and Anja S Göritz. 2021. A mobile VR-based respiratory biofeedback game to foster diaphragmatic breathing. *Virtual Reality* 25, 2 (2021), 539–552.

[63] Book Sadprasid, Anne Mei, Alex Mariakakis, Scott Bateman, and Fanny Chevalier. 2024. Leveraging idle games to incentivize intermittent and frequent practice of deep breathing. In *Proceedings of the CHI Conference on Human Factors in Computing Systems* (Honolulu HI USA). ACM, New York, NY, USA, 1–17.

[64] C Schäfer, M G Rosenblum, J Kurths, and H H Abel. 1998. Heartbeat synchronized with ventilation. *Nature* 392, 6673 (March 1998), 239–240.

[65] N Selvaraj, Ashok Kumar Jaryal, Jayasree Santhosh, K K Deepak, and Sneh Anand. 2008. Assessment of heart rate variability derived from finger-tip photoplethysmography as compared to electrocardiography. *Journal of medical engineering & technology* 32 (07 2008), 479–84. doi:10.1080/03091900701781317

[66] Fred Shaffer and J P Ginsberg. 2017. An overview of heart rate variability metrics and norms. *Front. Public Health* 5 (Sept. 2017).

[67] Chen-Hsuan (Iris) Shih, Naofumi Tomita, Yanick X. Lukic, Álvaro Hernández Reguera, Elgar Fleisch, and Tobias Kowatsch. 2020. Breeze: Smartphone-based Acoustic Real-time Detection of Breathing Phases for a Gamified Biofeedback Breathing Training. *Proc. ACM Interact. Mob. Wearable Ubiquitous Technol.* 3, 4, Article 152 (Sept. 2020), 30 pages. doi:10.1145/3369835

[68] Olivier Sibomana, Clyde Moono Hakayuwa, Abraham Obianke, Hubert Gahire, Jildas Munyantore, and Matimba Chilala. 2025. Diagnostic accuracy of ECG smart chest patches versus PPG smartwatches for atrial fibrillation detection: a systematic review and meta-analysis. *BMC Cardiovascular Disorders* 25 (02 2025), 132. doi:10.1186/s12872-025-04582-2

[69] Patrick R Steffen, Tara Austin, Andrea DeBarros, and Tracy Brown. 2017. The impact of resonance frequency breathing on measures of heart rate variability, blood pressure, and mood. *Front. Public Health* 5 (Aug. 2017), 222.

[70] Tibor Stracina, Marina Ronzhina, Richard Redina, and Marie Novakova. 2022. Golden standard or obsolete method? Review of ECG applications in clinical and experimental context. *Front. Physiol.* 13 (April 2022), 867033.

[71] Toshiyo Tamura, Yuka Maeda, Masaki Sekine, and Masaki Yoshida. 2014. Wearable photoplethysmographic sensors—past and present. *Electronics (Basel)* 3, 2 (April 2014), 282–302.

[72] Jiankai Tang, Zhe He, Mingyu Zhang, Wei Geng, Chengchi Zhou, Weinan Shi, Yuanchun Shi, and Yuntao Wang. 2025. τ-Ring: A Smart Ring Platform for Multimodal Physiological and Behavioral Sensing. In *Companion of the 2025 ACM International Joint Conference on Pervasive and Ubiquitous Computing*. 1271–1277.

[73] Grace Theodore, Jing-Yuan Huang, Lung-Pan Cheng, and Yi-Ping Hung. 2024. Breathm: A calm device with personalized slow breathing guidance. In *Extended Abstracts of the CHI Conference on Human Factors in Computing Systems* (Honolulu HI USA). ACM, New York, NY, USA.

[74] Tianben Wang, Daqing Zhang, Leye Wang, Yuanqing Zheng, Tao Gu, Bernadette Dorizzi, and Xingshe Zhou. 2019. Contactless Respiration Monitoring Using Ultrasound Signal With Off-the-Shelf Audio Devices. *IEEE Internet of Things Journal* 6, 2 (2019), 2959–2973. doi:10.1109/JIOT.2018.2877607

[75] Ruth Wells, Tim Outhred, James A J Heathers, Daniel S Quintana, and Andrew H Kemp. 2012. Matter over mind: a randomised-controlled trial of single-session biofeedback training on performance anxiety and heart rate variability in musicians. *PLoS One* 7, 10 (Oct. 2012), e46597.

[76] Margaret Wilson. 2002. Six views of embodied cognition. *Psychonomic bulletin & review* 9, 4 (2002), 625–636.

[77] Junfang Xie, Binyi Liu, and Mohamed Elsadek. 2021. How can flowers and their colors promote individuals' physiological and psychological states during the COVID-19 lockdown? *International Journal of Environmental Research and Public Health* 18, 19 (2021), 10258.

[78] Lin Xie, Mengjun Li, Shijie Dang, Chaomin Li, Xiaoni Wang, Binbin Liu, Mengqi Mei, and Jianbao Zhang. 2018. Impaired cardiorespiratory coupling in young normotensives with a family history of hypertension. *J. Hypertens.* 36, 11 (Nov. 2018), 2157–2167.

[79] Qiuxia Xu, Yingqi Gu, and Xizhe Hu. 2025. Brief interactive virtual reality mindfulness training with real-time biofeedback for anxiety reduction: A pilot study. *Appl. Psychophysiol. Biofeedback* (June 2025).

[80] Retory Yann, Pauline Niedzialkowski, Carole Picciotto, Marcel Bonay, and Michel Petitjean. 2016. New Respiratory Inductive Plethysmography (RIP) Method for Evaluating Ventilatory Adaptation during Mild Physical Activities. *PloS one* 11 (03 2016), e0151983. doi:10.1371/journal.pone.0151983

[81] Fumihiko Yasuma and Jun-Ichiro Hayano. 2004. Respiratory sinus arrhythmia. *Chest* 125, 2 (Feb. 2004), 683–690.

[82] Bin Yu, Pengcheng An, Sjoerd Hendriks, Ning Zhang, Loe Feijs, Min Li, and Jun Hu. 2021. ViBreathe: Heart rate variability enhanced respiration training for workaday stress management via an eyes-free tangible interface. *Int. J. Hum. Comput. Interact.* 37, 16 (Oct. 2021), 1551–1570.

[83] Bin Yu, Loe Feijs, Mathias Funk, and Jun Hu. 2015. Breathe with touch: A tactile interface for breathing assistance system. In *Human-Computer Interaction – INTERACT 2015*. Springer International Publishing, Cham, 45–52.

[84] Yangbo Yuan, Hao Chen, Hongcheng Xu, Yujian Jin, Gang Chen, Weihao Zheng, Weidong Wang, Yuejiao Wang, and Libo Gao. 2022. Highly sensitive and wearable bionic piezoelectric sensor for human respiratory monitoring. *Sensors and Actuators A: Physical* 345 (2022), 113818. doi:10.1016/j.sna.2022.113818

[85] Yifan Zhang, Shuang Song, Rik Vullings, Dwaipayan Biswas, Neide Simões-Capela, Nick van Helleputte, Chris van Hoof, and Willemijn Groenendaal. 2019. Motion Artifact Reduction for Wrist-Worn Photoplethysmograph Sensors Based on Different Wavelengths. *Sensors* 19, 3 (2019). doi:10.3390/s19030673

A Use of Generative AI Tools

For this work, generative AI tools were used in a limited and responsible manner:

- **Text:** ChatGPT 5.0 was used only for grammar checking and language polishing to improve the clarity and readability of the manuscript.
- **Figures:** We use ChatGPT 5.0 for generating illustrative simulated character images in Figure 1, 5 and 7, to visually support the manuscript.

No AI-generated content was used to generate experimental data, results, or any interpretive content.